ACCELERATED PUBLICATION

This paper is available online at www.jbc.org

THE JOURNAL OF BIOLOGICAL CHEMISTRY VOL. 283, NO. 35, pp. 23510–23513, August 29, 2008

Monomeric CFTR in Plasma Membranes in Live Cells Revealed by Single Molecule Fluorescence Imaging*[S]

Received for publication, May 15, 2008, and in revised form, June 19, 2008
Published, JBC Papers in Press, July 9, 2008, DOI 10.1074/jbc.C800100200

Peter M. Haggie[1] **and A. S. Verkman**

From the Departments of Medicine and Physiology, University of California, San Francisco, California, 94143

The cystic fibrosis transmembrane conductance regulator (CFTR) is a cAMP-regulated chloride channel. There is indirect and conflicting evidence about whether CFTR exists in cell membranes as monomers, dimers, or higher order oligomers. We measured fluorescence intensities and photobleaching dynamics of distinct fluorescent spots in cells expressing functional CFTR-green fluorescent protein (GFP) chimeras. Intensity analysis of GFP-labeled CFTR in live cells showed single-component distributions with mean intensity equal to that of purified monomeric GFP, indicating monomeric CFTR in cell membranes. Fluorescent spots showed single-step photobleaching, independently verifying that CFTR is monomeric. Results did not depend on whether GFP was added to the CFTR N terminus or fourth extracellular loop or on whether CFTR chloride conductance was stimulated by cAMP agonists. Control measurements with a CFTR chimera containing two GFPs showed two-step photobleaching and a single-component intensity distribution with mean intensity twice that of monomeric GFP. These results provide direct evidence for monomeric CFTR in live cells.

The cystic fibrosis transmembrane conductance regulator (CFTR)[2] is a member of the ATP-binding cassette protein family that forms cAMP-regulated chloride channels (1). CFTR is expressed in epithelial cells in the airways, pancreas, intestine, and other tissues (2). Loss-of-function mutations in CFTR cause the hereditary lethal disease cystic fibrosis, in which chronic lung infection produces morbidity and mortality (1, 2). Excessive CFTR activity in the intestine in response to bacterial enterotoxins produces secretory diarrheas (3, 4). There is considerable interest in CFTR structure and assembly in cell membranes as CFTR is an important drug target for therapy of cystic fibrosis, secretory diarrheas, and polycystic kidney disease (3, 5–7).

The assembly state of CFTR has been controversial, with indirect evidence reported for CFTR monomers, dimers, and mixed monomers/dimers. Patch clamp analysis of constructs containing linked wild-type (WT) CFTRs or WT and mutant CFTRs suggested that two CFTR polypeptides form a single chloride conductance pathway (8). Conflicting data from reconstituted membranes containing WT and mutant CFTRs did not reveal intermediary conductance states, consistent with independently functioning CFTR monomers (9). Electron crystallography has indicated that CFTR is a monomer with two conformations, likely the open and closed channel states (10). These data are in accord with high resolution crystal structures of bacterial ATP-binding cassette-type transporters showing unit cells containing two transmembrane-nucleotide binding domains (11). Biochemical approaches including velocity-gradient centrifugation, coimmunoprecipitation, gel filtration, and cross-linking have generated conflicting data suggesting monomeric CFTR (9, 12), dimeric CFTR (13), and mixed monomeric/dimeric CFTR (14, 15). Data supporting dimeric CFTR have also come from patch clamp of CFTR in the presence of the PDZ domain proteins CAP70 and EBP50 (16–18), from freeze-fracture electron microscopy (19), and from atomic force microscopy (20). However, the interpretation of many of these studies is not clear-cut in distinguishing CFTR monomers from dimers. Multistate single channel data are subject to alternate interpretations, native CFTR quaternary structure may not be preserved during detergent solubilization or crystallization, and similar CFTR dimensions were found but interpreted differently in freeze-fracture electron microscopy (~9 nm, interpreted as dimeric CFTR (19)) and electron crystallography (~7 nm, interpreted as monomeric CFTR (10)).

Here, we determined CFTR assembly state in intact membranes of live cells using single molecule fluorescence imaging. Single molecule fluorescence methods have been applied previously to determine the subunit composition of membrane proteins (21), synaptic proteins (22), and bacterial flagellar proteins (23). Intensity and photobleaching measurement on functional CFTR-GFP chimeras provided direct evidence for exclusively monomeric CFTR in live cell membranes.

EXPERIMENTAL PROCEDURES

Cell Culture and Transfections—COS7 and CHO K1 cells were cultured using standard methods in Dulbecco's modified Eagle's medium H21 without phenol red, 10% fetal bovine serum, 2 mM glutamine, non-essential amino acids, 100 units/ml penicillin, and 100 μg/ml streptomycin. Cells were transfected using Lipofectamine™ 2000 (Invitrogen™) according to the manufacturer's directions, and transfected

* This work was supported, in whole or in part, by National Institutes of Health Grants HL73856, EB00415, HL59198, DK35124, EY13574, DK72517, and DK081355. This work was also supported by Research Development Program Grant R613 from the Cystic Fibrosis Foundation, and Beginning Grant-in-Aid 0765070Y from the American Heart Association. The costs of publication of this article were defrayed in part by the payment of page charges. This article must therefore be hereby marked "*advertisement*" in accordance with 18 U.S.C. Section 1734 solely to indicate this fact.

[S] The on-line version of this article (available at http://www.jbc.org) contains a supplemental movie.

[1] To whom correspondence should be addressed: Tel: 415-476-8530; Fax: 415-665-3847; E-mail: peter.haggie@ucsf.edu.

[2] The abbreviations used are: CFTR, cystic fibrosis transmembrane conductance regulator; GFP, green fluorescent protein; EYFP, enhanced yellow fluorescent protein; CHO, Chinese hamster ovary; TIRF, total internal reflection fluorescence; PBS, phosphate-buffered saline; WT, wild type.

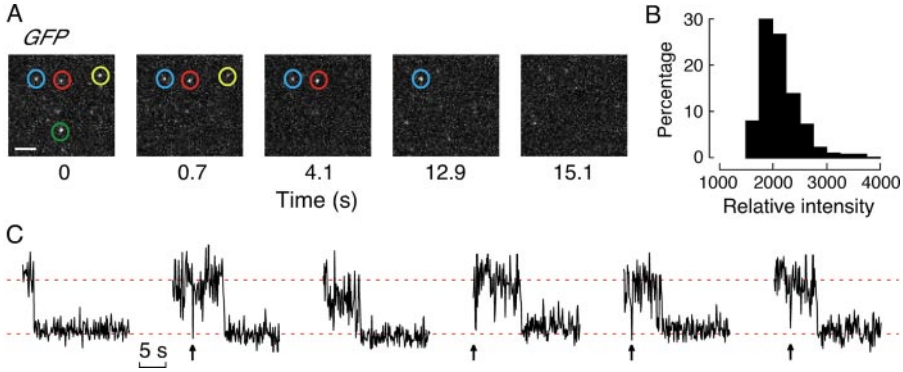

FIGURE 1. **Total internal reflection fluorescence imaging of purified monomeric GFP.** *A*, representative frames from an image sequence of GFP bleaching with individual GFP molecules highlighted by *colored circles*. Times shown are relative to the initial image. Data were acquired at 10 Hz using a 100-ms integration time (*scale bar*, 2 μm). *B*, histogram of averaged background-corrected, area-integrated fluorescence intensities of individual GFP molecules. Resolvable fluorescent spots that remained fluorescent for at least 3 s prior to bleaching were analyzed. *C*, gallery of photobleaching events showing one-step photobleaching of individual GFP molecules. *Arrows* correspond to GFP blinking events.

cells were passaged over 7–12 days to reduce CFTR expression. Plasmid constructs expressing GFP fused to the N terminus of wild-type CFTR (GFP-CFTR) and CFTR mutated to remove the C-terminal PDZ-binding domain (GFP-CFTR-ΔTRL) have been described (24, 25). A second N terminus GFP-CFTR construct with a shorter 16-amino acid linker was also studied (GFP_{16aa}-CFTR, provided by Dr. G. Lukacs). To label CFTR with a GFP moiety at an alternative, extracellular site (CFTR-GFP_{ext}), EcoRV and KpnI sites were engineered into the fourth extracellular loop of CFTR (between the CFTR glycosylation sites), and the GFP coding sequence was ligated in-frame with the CFTR sequence. To generate CFTR labeled with two GFP moieties (CFTR-GFP2), a second GFP moiety was ligated into NheI sites engineered into the fourth extracellular loop of CFTR labeled at the C terminus with a GFP (26). All constructs were confirmed by sequence analysis. His_6-tagged unconjugated GFP was purified by nickel affinity chromatography and confirmed to be homogeneous by SDS-PAGE.

Microscopy and Image Analysis—Single molecule fluorescence imaging was performed by objective-type total internal reflection fluorescence (TIRF) on a Nikon Eclipse TE2000E microscope equipped with infrared autofocus, ×100, 1.49 numerical aperture (NA) Apo TIRF objective, Nikon TIRF attachment, Photometrics QuantEM 512SC CCD camera, and Spectra-Physics Advantage 161C 10 milliwatt argon ion laser (coupled to fiber optic via a quarter wave plate). Filters included a Z488/10x excitation filter, Z488RDC dichroic mirror, and ET525/50m emission filter (Chroma). All image sequences were acquired at 10 frames per s using identical CCD settings in the central region (~20 × 20 μm) of the CCD chip. For imaging, cells were grown on 18-mm diameter coverglasses, mounted in a custom chamber with PBS containing 6 mM glucose and 1.1 mM sodium pyruvate, and maintained at 37 °C by a Harvard Apparatus microincubator. Single molecules of purified monomeric GFP were imaged on coverglasses in PBS (pH 7.4). Semiautomated image analysis was done using algorithms developed for the IDL platform (Research Systems, Inc. (26)) and in NIS Elements AR (Nikon).

CFTR Halide Transport Assay—Transport was assayed in COS7 cells co-transfected with a CFTR-GFP construct and the halide-sensitive EYFP-H148Q protein (27). Cells were imaged 1 day after transfection on a Nikon TE2000E microscope using a Nikon ×20, 0.75 NA S Fluor objective, 31001 filter set (Chroma), and QuantEM 512SC CCD camera. Cells were bathed for 5 min in PBS containing 20 μM forskolin prior to solution exchange to give a 100 mM iodide gradient, as described (27). The kinetics of single cell fluorescence was analyzed using NIS Elements AR software. In some experiments, forskolin was omitted or CFTR inhibitor ($CFTR_{inh}$-172, 10 μM) was included. Control experiments indicated that GFP fluorescence from the CFTR chimeras did not contribute significantly to measured signal intensities.

RESULTS AND DISCUSSION

Our strategy to determine CFTR oligomeric state was to image GFP-labeled CFTR chimeras in plasma membranes of live cells in which the fluorescence associated with individual CFTR monomers/oligomers was seen as diffraction-limited spots. Dimeric CFTR would have twice the intensity of monomeric CFTR and show two-step rather than one-step photobleaching. The genetic attachment of GFP to CFTR obviates nonspecific labeling as might occur with antibody labeling and guarantees that each CFTR polypeptide is labeled with one and only one fluorophore. We used TIRF Illumination, which produces an exponentially decreasing excitation field of ~150 nm at the interface between media of high and low refractive indices (28). TIRF produces high signal-to-noise ratios for single molecule imaging of plasma membrane proteins.

Our system was validated using purified GFP monomers on coverglasses that were visible by TIRF illumination as discrete fluorescent spots (Fig. 1*A*). Over time, each fluorescent spot disappeared because of photobleaching. The background-corrected, area-integrated fluorescence intensities of individual spots produced a unimodal distribution (Fig. 1*B*). Factors that contribute to the finite width of the intensity distribution include Poisson noise, GFP blinking, and illumination inhomogeneity (29, 30). To confirm that single GFP molecules were being imaged, we measured the time course of fluorescence intensity of individual fluorescent spots. As expected for single fluorophores, one-step photobleaching was observed in which the fluorescence intensity was reduced to background within one image frame (Fig. 1*C*). Further, in some instances, GFP blinking was seen in which signal intensity decreased briefly to background before returning to original levels (Fig. 1*C*, *arrows*).

To determine CFTR oligomeric state in live cells, GFP-labeled CFTR constructs were expressed in cells lacking endogenous CFTR, which could associate with the tagged CFTR and confound data interpretation. We first studied a CFTR chimera

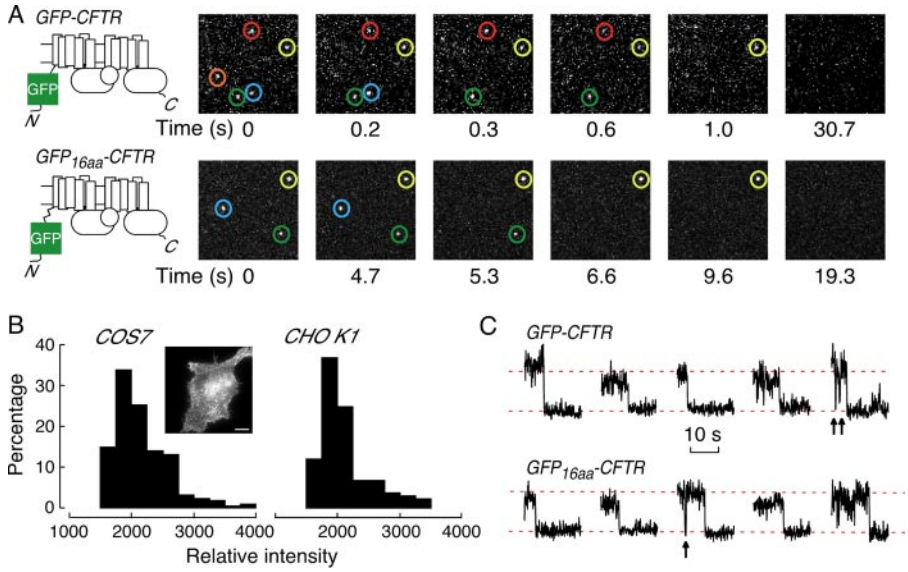

FIGURE 2. **Total internal reflection imaging of GFP-labeled CFTR in the plasma membrane of live cells.** *A*, N-terminal GFP-labeled CFTR constructs containing linkers of length 23 (*top*) and 16 (*bottom*) amino acids. Representative frames from image sequences for each GFP-labeled CFTR chimera expressed in COS7 cells are shown with individual fluorescent spots highlighted by *colored circles*. Data were acquired at 10 Hz using 100-ms integration times. *N*, N terminus; *C*, C terminus. *B*, histograms of area-integrated, background-corrected fluorescent intensities of fluorescent spots in COS7 (*left*) and CHO K1 (*right*) cells expressing GFP-CFTR. *Inset*, TIRF image of COS7 cell expressing a high level of GFP-CFTR (*scale bar*, 10 μm). *C*, time course of fluorescence of individual spots for the 23- (*top*) and 16- (*bottom*) amino acid linker CFTR constructs in COS7 cells. One-step photobleaching and blinking (*arrows*) verify imaging of individual fluorophores.

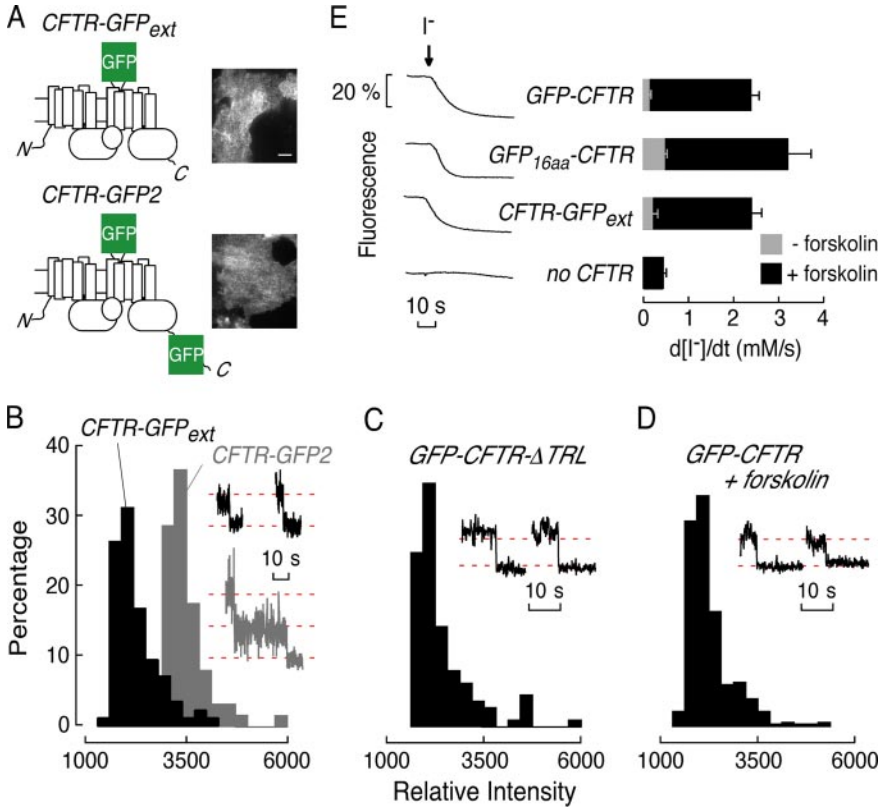

FIGURE 3. **Evidence for monomeric CFTR in live cells, independent of CFTR phosphorylation state and PDZ-interactions.** *A*, GFP-labeled CFTR chimeras with GFP in the fourth extracellular loop (CFTR-GFP$_{ext}$, *top left*) and CFTR labeled with two GFPs (CFTR-GFP2, *bottom left*). TIRF images of COS7 cell expressing high levels of CFTR-GFP$_{ext}$ (*top right*) and CFTR-GFP2 (*bottom right*) (*scale bar*, 10 μm) are shown. *N*, N terminus; *C*, C terminus. *B–D*, histograms of fluorescence intensities in COS7 cells expressing CFTR-GFP$_{ext}$ (*B*, *black*), CFTR-GFP2 (*B*, *gray*), GFP-CFTR-ΔTRL (*C*), and GFP-CFTR after forskolin stimulation (*D*). *Insets* show representative photobleaching of single spots. *E*, iodide transport assay of indicated GFP-labeled CFTR constructs and non-transfected cells. Examples of single cell fluorescence (shown with forskolin, *left*) and average iodine influx rates (*right*, mean ± S.E.) are displayed.

in which GFP was fused to the N terminus of CFTR with a 23-amino acid linker (GFP-CFTR, Fig. 2*A*, *top*). The GFP-CFTR chimera is fully functional and processed like native CFTR (24, 31).

TIRF imaging of cells expressing high levels of GFP-CFTR revealed a fluorescence pattern characteristic of CFTR, a protein that is endocytosed and recycled (32, 33), with labeling of the plasma membrane and subplasma membrane endosomes/exocytic vesicles (Fig. 2*B*, *inset, left*). After passaging cells to reduce GFP-CFTR expression, discrete fluorescent spots were seen in the plasma membrane of COS7 cells (Fig. 2*A*, *top*). As found for purified monomer GFP, individual fluorescent spots in cells expressing GFP-CFTR disappeared over time due to photobleaching. The fluorescence intensities of single spots showed unimodal distributions (Fig. 2*B*) of similar absolute intensity to that of purified monomeric GFP (Fig. 1*B*). One-step photobleaching confirmed monomeric GFP-CFTR in COS7 cells (Fig. 2*C*, *top*, see also supplemental movie 1). We also studied a second chimera having a shorter, 16-amino acid linker between the N-terminal GFP and CFTR moieties (GFP$_{16aa}$-CFTR). As with GFP-CFTR, individual fluorescent spots were seen in the plasma membrane of COS7 cells (Fig. 2*A*, *bottom*) of equal intensity to purified GFP (data not shown) that showed one-step photobleaching (Fig. 2*C*, *bottom*). We also expressed GFP-CFTR in a different cell type (CHO K1 cells). The fluorescence intensity of individual spots was similar in CHO K1 and COS7 cells (Fig. 2*B*), with all spots showing one-step photobleaching (data not shown). In no instance for either construct or cell type was two-step photobleaching seen.

To confirm that GFP fusion to the CFTR N terminus does not prevent CFTR oligomerization, we generated a chimera in which the GFP moiety was inserted into the fourth extracellular loop of CFTR (CFTR-GFP$_{ext}$, Fig. 3*A*, *top left*). This site

was previously identified to be amenable to insertions (*e.g.* a triplet hemagglutinin epitope tag) and does not interfere with C-terminal PDZ interactions (26). TIRF imaging of CFTR-GFP_{ext} at high expression levels revealed a fluorescence pattern similar to that of GFP-CFTR, indicating plasma membrane trafficking (Fig. 3*A*, *top right*). As with N-terminal GFP fusions, the fluorescence intensity associated with individual spots in CFTR-GFP_{ext}-expressing cells showed a unimodal distribution (Fig. 3*B*, *black histogram*) with single-step photobleaching (Fig. 3*B*, *inset*, *black traces*).

To verify that we could distinguish a putative CFTR dimer, each CFTR was labeled with two GFP moieties (CFTR-GFP2, Fig. 3*A*, *bottom left*). As anticipated, fluorescence of individual spots in cells expressing CFTR-GFP2 was unimodal and ~2-fold greater than that of GFP-labeled CFTR chimeras containing one GFP, and two-step photobleaching was observed (Fig. 3*B*, *gray histogram* and *trace*).

Additionally, the fluorescence properties of GFP-CFTR lacking its C-terminal PDZ-binding domain (GFP-CFTR-ΔTRL) indicated a monomeric state (Fig. 3*C*). CFTR channels remained in a monomeric state as well upon forskolin addition (Fig. 3*D*).

Last, using an established fluorescence measurement method (27), we verified that the CFTR chimeras containing single GFP moieties were functional halide transporters. COS7 cells were co-transfected with halide-sensitive fluorescent protein EYFP-H148Q and each of the CFTR constructs. Cellular fluorescence decreased by 20–30% in response to a 100 mM iodide gradient in cells expressing GFP-CFTR (a chimera previously shown to have normal CFTR activity (24, 31)), GFP_{16aa}-CFTR, and CFTR-GFP_{ext} (Fig. 3*E*). Fluorescence was not reduced in non-transfected cells or without forskolin (Fig. 3*E*) or in the presence of CFTR inhibitor (not shown).

Taken together, these studies provide compelling evidence for monomeric CFTR in plasma membranes of live cells. As such, a single CFTR polypeptide is sufficient for the conductance of chloride and bicarbonate ions. Neither CFTR activation by protein kinase A nor PDZ domain deletion altered its oligomeric state. The novel use of complementary single-spot intensity and photobleaching analysis provided clear-cut evidence for exclusively monomeric CFTR in the cell systems studied here. Whether CFTR could form dimers in some cell systems and under some conditions seems unlikely but cannot be proven definitively at this time.

Acknowledgments—We thank Dr. J. M. Crane for assistance with analysis algorithms. Parts of this study were conducted using facilities at the Nikon Imaging Center, University of California, San Francisco (UCSF) and the Biological Imaging Development Center, UCSF.

REFERENCES

1. Gadsby, D. C., Vergani, P., and Csanády, L. (2006) *Nature* **440,** 477–483
2. Rowe, S. M., Miller, S., and Sorscher, E. (2005) *N. Engl. J. Med.* **352,** 1992–2001
3. Kunzelmann, K., and Mall, M. (2002) *Physiol. Rev.* **82,** 245–289
4. Thiagarajah, J. R., and Verkman, A. S. (2005) *Trends Pharmacol. Sci.* **26,** 172–175
5. Thiagarajah, J. R., and Verkman, A. S. (2003) *Curr. Opin. Pharmacol.* **3,** 594–599
6. Verkman, A. S. (2004) *Curr. Opin. Nephrol. Hypertens.* **13,** 563–568
7. Verkman, A. S., Lukacs, G. L., and Galietta, L. J. (2006) *Curr. Pharm. Des.* **12,** 2235–2247
8. Zerhusen, B., Zhao, J., Xie, J., Davis, P. B., and Ma, J. (1999) *J. Biol. Chem.* **274,** 7627–7630
9. Chen, J.-H., Chang, X.-B., Aleksandrov, A. A., and Riordan, J. R. (2002) *J. Membr. Biol.* **188,** 55–71
10. Rosenberg, M. F., Kamis, A. B., Aleksandrov, L. A., Ford, R. C., and Riordan, J. R. (2004) *J. Biol. Chem.* **279,** 39051–39057
11. Hollenstein, K., Dawson, R. J., and Locher, K. P. (2007) *Curr. Opin. Struct. Biol.* **17,** 412–418
12. Marshall, J., Fang, S., Ostegaard, L. S., O'Riordan, C. R., Ferrara, D., Amara, J. F., Hoppe, H., IV, Scheule, R. K., Welsh, M. J., Smith, A. E., and Cheng, S. H. (1994) *J. Biol. Chem.* **269,** 2987–2995
13. Li, C., Roy, K., Dandridge, K., and Naren, A. P. (2004) *J. Biol. Chem.* **279,** 24673–24684
14. Ramjeesingh, M., Li, C., Kogan, I., Wang, Y., Huan, L.-J., and Bear, C. E. (2001) *Biochemistry* **40,** 10700–10706
15. Ramjeesingh, M., Kidd, J. F., Huan, L. J., Wang, Y., and Bear, C. E. (2003) *Biochem. J.* **374,** 793–797
16. Wang, S., Yue, H., Derin, R. B., Guggino, W. B., and Li, M. (2000) *Cell* **103,** 169–179
17. Raghuram, V., Mak, D.-O. D., and Foskett, J. K. (2001) *Proc. Natl. Acad. Sci. U. S. A.* **98,** 1300–1305
18. Raghuram, V., Hormouth, H., and Foskett, J. K. (2003) *Proc. Natl. Acad. Sci. U. S. A.* **100,** 9620–9625
19. Eskandari, S., Wright, E. M., Kreman, M., Starace, D. M., and Zampighi, G. A. (1998) *Proc. Natl. Acad. Sci.* **95,** 11235–11240
20. Schillers, H., Shahin, V., Albermann, L., Schafer, C., and Oberleithner, H. (2004) *Cell Physiol. Biochem.* **14,** 1–10
21. Ulbrich, M. H., and Isacoff, E. Y. (2007) *Nat. Meth.* **4,** 319–321
22. Sugiyama, Y., Kawabata, I., Sobue, K., and Okabe, S. (2005) *Nat. Meth.* **2,** 677–684
23. Leake, M. C., Chandler, J. H., Wadhams, G. H., Bai, F., Berry, R. M., and Armitage, J. P. (2006) *Nature* **443,** 355–358
24. Moyer, B. D., Denton, J., Karlson, K. H., Reynolds, D., Wang, S. S., Mickle, J. E., Milewski, H., Cutting, G. R., Guggino, W. B., Li, M., and Stanton, B. A. (1999) *J. Clin. Investig.* **104,** 1353–1361
25. Haggie, P., Stanton, B. A., and Verkman, A. S. (2004) *J. Biol. Chem.* **279,** 5494–5500
26. Haggie, P. M., Kim, J. K., Lukacs, G. L., and Verkman, A. S. (2006) *Mol. Biol. Cell* **17,** 4937–4945
27. Galietta, L. J., Springsteel, M. F., Eda, M., Niedzinski, E. J., By, K., Haddadin, M. J., Kurth, M. J., Nantz, M. H., and Verkman, A. S. (2001) *J. Biol. Chem.* **276,** 19723–19728
28. Steyer, J. A., and Almers, W. A. (2001) *Nat. Rev. Mol. Cell Biol.* **2,** 268–276
29. Dickson, R. M., Cubitt, A. B., Tsien, R. Y., and Moerner, W. E. (1997) *Nature* **338,** 355–358
30. Haupts, U., Maiti, S., Schwille, P., and Webb, W. W. (1998) *Proc. Natl. Acad. Sci. U. S. A.* **95,** 13573–13578
31. Moyer, B. D., Loffing, J., Schwiebert, E. M., Loffing-Cueni, D., Halpin, P. A., Karlson, K. H., Ismailov, I. I., Guggino, W. B., Langford, G. M., and Stanton, B. A. (1998) *J. Biol. Chem.* **273,** 21759–21768
32. Lukacs, G. L., Segal, G., Kartner, N., Grinstein, S., and Zhang, F. (1997) *Biochem. J.* **328,** 353–361
33. Sharma, M., Pampinella, F., Nemes, C., Benharouga, M., So, J., Du, K., Bache, K. G., Papsin, B., Zerangue, N., Stenmark, H., and Lukacs, G. L. (2004) *J. Cell Biol.* **164,** 923–933